U.S. DEPARTMENT OF THE INTERIOR

U.S. GEOLOGICAL SURVEY

SECONDARY MINERALOGY OF ALTERED ROCKS, SUMMITVILLE MINE, COLORADO

by

Marta J.K. Flohr[1], Roberta G. Dillenburg[1], Gordon L. Nord, Jr.[1], and Geoffrey S. Plumlee[2]

Open-File Report 95-808

[1] U.S. Geological Survey
National Center, MS 959
Reston, VA 22092

[2] U.S. Geological Survey
Denver Federal Center, MS 973
Denver, CO 80225

CONTENTS

PAGE

Introduction 1
Methods 2
Samples 2
Discussion 3
Conclusions 8
Acknowledgments 8
References Cited 9

ILLUSTRATIONS

Figure 1. Simplified map of the Summitville mine site 11
Figure 2. Encrustation of hinsdalite and a Cu-sulfate mineral on chalcocite 12
Figure 3A. Hinsdalite after alunite in chalcocite-rich rock 13
Figure 3B. Zoned hinsdalite 13
Figure 4. Hinsdalite-chalcocite intergrowth and relict aluminous phosphate-sulfate minerals 14
Figure 5. Encrustation of secondary jarosite 15
Figure 6A-E. Examples of bacterial-type morphologies in Fe-rich stalactite 16
Figure 7A. Fe- and Sb-rich bacterial-type material 17
Figure 7B. Fe- and As-rich bacterial-type material 17
Figure 8A-B. Rosettes of nodular gypsum encrustation. 18
Figure 9A-B. Plant material 19

TABLES

Table 1. Ideal chemical formulas of minerals identified in this study from the Summitville site 20
Table 2. Summary of minerals identified in samples from the Summitville site . . . 21

APPENDIX

Appendix A. Sample descriptions 23

INTRODUCTION

The Summitville mine (Fig. 1) was developed in an epithermal acid-sulfate Au-Ag-Cu deposit that is hosted by the quartz latite lavas of the South Mountain volcanic dome. It is located at an elevation of about 3800 meters (11,500 ft) in the southeastern part of the San Juan volcanic field, Colorado. The Summitville mine has been the focus of attention because of environmental problems resulting from open-pit mining activities that occurred from 1984 to 1992. The environmental problems included leakage of cyanide solutions from a heap leach pad and drainage of acid- and metal-rich waters into the Wightman Fork of the Alamosa River, which drains into agricultural lands of the southwest San Luis Valley. In the past several years, the U.S. Geological Survey has had an extensive program to study different aspects of the environmental changes caused by this mining activity (Plumlee and Edelman, 1995).

This report presents the characterization of secondary minerals that form as the result of the oxidation of sulfide minerals and evaporation of acid mine waters at the Summitville mine site. Open-pit mining at the site exposed abundant sulfide-bearing rocks. Subsequent oxidation of the sulfide minerals by oxygenated ground waters generated highly acidic, metalliferous drainage waters; evaporation of these waters leaves behind a variety of secondary salts that host a variety of metals and other elements (e.g., Fe, Cu, Zn, Al, As, Pb, S) (Plumlee and others, 1995a). Understanding the geochemical behavior of these elements contributes to the understanding of metal mobility and helps us assess the role that secondary minerals play in controlling mine drainage chemistry. Plumlee and others (1995a) reported that seasonal increases in the metal load of drainage waters is attributed to the dissolution of some soluble secondary minerals during periods of snowmelt runoff or periods of high precipitation. However, secondary minerals and bacterially-precipitated material that host potentially toxic elements may be relatively insoluble and this prevents liberation of their contained elements into the environment. In the samples examined in this study, we have also identified and characterized the minerals that constitute the clay- and (or) sulfide-rich rocks that host the secondary minerals. By knowing the distribution of major and minor elements in both the secondary and earlier-formed primary minerals, we can better understand the chemical budget of the system.

A summary of the early mining of gold at the site is given by Gray and others (1993). Gray and others (1994) and Plumlee and Edelman (1995) detailed the environmental aspects of recent mining at the Summitville site which are briefly summarized here. From 1985 to 1992 Summitville Consolidated Mining Company, Inc. (SCMCI) operated an open-pit gold mine at Summitville. The mining process exposed sulfide ore; as a result, acid- and metal-rich drainage from the site into Wightman Fork increased. Gold was extracted from crushed ore by a heap leach process, which continued until 1992; crushed ore was placed on a heap leach pad, underlain by a protective liner, and was then sprinkled with a weak cyanide solution. Gold was extracted from the ore by the cyanide and then recovered from the cyanide solution by a chemical process. Leakage of the cyanide solution beneath the leach pad occurred and these solutions mixed with acid ground waters from the waste dump up gradient. SCMCI began remediation, but abandoned these efforts in December, 1992 when the company declared bankruptcy. The Environmental Protection Agency (EPA) took over the site under the EPA Superfund Emergency Response authority and it was added to the EPA National Priorities List in May, 1994.

Stoffregen (1987), Gray and others (1993), and Gray and Coolbaugh (1994) provided detailed descriptions of the geology and mineralization of the Summitville site.

Summaries of earlier studies of the deposit are given in these two reports. Gray and Coolbaugh (1994) identified six stages in the development of the Summitville deposit: (1) acid-sulfate alteration, (2) Cu-sulfide mineralization and Au mineralization, (3) hydrothermal brecciation, (4) formation of base metal sulfide-bearing barite veins, (5) kaolinite matrix brecciation, and (6) supergene alteration. The alteration zones (vuggy silica, quartz-alunite, quartz-kaolinite, argillic, and propylitic) developed during the intense early acid-sulfate alteration of the host quartz latite of the South Mountain volcanic dome. Sulfide mineralization followed, with the deposition of enargite, luzonite, covellite, pyrite, native sulfur, marcasite, sphalerite, native gold, barite, and galena. The samples described in this report include several of the altered and sulfide-mineralized rock types generated during the early development of the Summitville deposit.

METHODS

Relict primary minerals, minerals formed during different stages of weathering of the deposit, and secondary minerals (Table 1) were identified by X-ray powder diffraction (XRD). Their chemical compositions were qualitatively characterized by use of the X-ray energy-dispersive analysis system (EDS) on a JEOL JSM-840 scanning electron microscope (SEM). Selected minerals were analyzed on the SEM using a standardless software analysis routine that uses a ZAF correction procedure (Princeton Gamma-Tech, Inc., 1994). These analyses are regarded as semi-quantitative, based on analyses of well-characterized mineral standards. Polished slabs and thin sections of sulfide ore, quartz-alunite rock, and vuggy silica also were examined using the petrographic microscope.

Standard XRD procedures were used. Bulk samples and separates, hand picked under a binocular microscope, were analyzed. Because the secondary minerals rarely occur as discreet monomineralic aggregates or segregations and because the minerals are typically fine grained, it was usually not possible to obtain pure separates of individual phases. All samples were ground in acetone or isopropanol and prepared as either smear mounts or as slurries on quartz plates. Nickel filtered CuKα X-ray radiation was used. The X-ray unit was operated at 40 kV and 30 mA. X-ray diffraction patterns were obtained as either scans, typically run at 1° 2θ per minute from 70° to 4° 2θ, or as step scans run at 100 steps per degree 2θ, with a count time of 1.2 seconds per step.

The SEM was operated at an accelerating voltage of 20 kV and a specimen current of about 1 to 2 nA. All samples were carbon coated. Isolation of fine-grained secondary minerals that occur disseminated in clay-rich altered rocks was facilitated by disaggregating the sample in isopropanol and allowing the solution to dry on a polycarbonate membrane (0.2 μm pore size), which was then mounted on conductive carbon tape on a glass slide.

One sample was examined in a JEOL 200B scanning transmission electron microscope (STEM) at an operating voltage of 200 keV. The material was dispersed on a formvar coated 200 mesh copper grid and was carbon coated.

SAMPLES

The fifteen samples studied (Table 2, Appendix A) were collected by one of us (G.S.P.) from different areas within the Summitville mine site (Fig. 1). These areas include the South Pit (SP-1), the North Pit (NP1-S5) (both from within the open pit area), the top of the clay ore stockpile and the mudflats at the top of the clay ore stock pile (TCOSP and MFCOSP, respectively), the Cropsy waste dump (CW2, CW3), the North Dexter vein

(ND1, ND2, ND3-I, ND3-II), the North waste dump (NDP), the Bank Seep in Area L Seep (SAL-BS), and the Reynolds adit (AD-1500). Two additional samples were also studied: one of vuggy silica (SO) and the other of a treated sample (H_2Ot) that was collected downstream from the water treatment plant. At the water treatment plant, sodium bisulfide and other compounds (Na- and Ca-bearing) are added to the acid mine waters to raise the pH of these waters. The areas from which the samples were collected represent different geochemical environments within the mine site. Plumlee and others (1995a) demonstrated that pH and composition of waters obtained from adits, puddles, and seeps from these areas and from other areas within the mine site are different. For example, they reported pH values of 1.7 to 3.3. Samples included for mineralogical study were chosen to complement water analyses and leaching experiments conducted on the samples (Plumlee and others, 1995a) and to identify the variety of secondary phases present at the site.

DISCUSSION

Mineralogy

The secondary minerals (Table 1) identified in this study are dominated by sulfate minerals, including chalcanthite, brochantite, posnjakite, melanterite, alunogen, halotrichite, gypsum, alunite, and jarosite. Sodium sulfate and sideronatrite were found in a sample (H_2Ot) collected downstream from the water treatment plant. Goethite, scorodite, poorly crystalline Fe-rich crusts, and three different Fe-rich materials that may be of bacterial origin were also identified. The secondary minerals form efflorescent crusts, thin coatings, and fracture fillings. Some of the secondary minerals formed as the result of long-term weathering of the deposit prior to mining, whereas others formed as a result of mining activities; these two different groups of minerals are referred to as pre-mining and post-mining secondary minerals (Table 1), respectively, following the classification of Plumlee and others (1995b). Textural data indicate that some of the secondary minerals, such as jarosite and, possibly, ferrihydrite, formed as both pre- and post-mining minerals. In addition to forming during argillic alteration, alunite is also a secondary mineral, but whether it formed prior to or as a result of mining activities is not clear. "Limonite" was also described as a pre-mining secondary phase and probably includes at least some of the poorly crystalline Fe-rich crusts and suspected bacterial materials described here (for example, Patton, 1917, described limonitic stalactites, which may be similar to stalactite AD1500, Appendix A).

All the secondary minerals identified from the Summitville mine site thus far have been reported from other areas of acid drainage. Alpers and others (1994) and Jambor (1994) provided excellent summaries of the diverse secondary mineralogy encountered at mine sites.

The compositions of the secondary minerals are governed by the availability of elements from the sulfide ore minerals and gangue minerals and the stability of these minerals. Sulfur, Cu, Fe, As, Sb, Zn, and Pb are derived from the weathering of the sulfide minerals [Table 1; also, see Gray and Coolbaugh (1994) for a more complete description of the mineralogy of the site, as Table 1 only lists those minerals identified in the small sample suite described herein]. Aluminum, Mg, and Fe are derived from the clay minerals, chlorite, and (or) biotite. The dissolution of feldspar minerals provides Al, K, Na, and Ca. The association of hydrated Fe-sulfate minerals, such as melanterite, with the Al-sulfates halotrichite and alunogen has been reported from numerous other areas of acid drainage where aluminous minerals are associated with Fe-sulfides (Flohr and others, 1995, and

references therein). The different habits and compositions exhibited by halotrichite in a single sample (i.e., sample CW2) is apparently common and reflects progressive deposition of the halotrichite as efflorescent crusts develop.

Sulfate and phosphate-sulfate minerals of the alunite-jarosite group. The alkali sulfate and aluminous phosphate-sulfate (APS) minerals from Summitville (Table 1) comprise a compositionally diverse group that formed during different stages in the development of the deposit. Whereas the paragenesis of some of these minerals at the Summitville mine is understood, the formation of hinsdalite, a Pb-bearing APS mineral, has been less clear. APS minerals, principally those of the svanbergite-woodhouseite solid solution series, replaced primary igneous apatite during advanced stages of argillic alteration (Stoffregen and Alpers, 1987). Alunite, which occurs in quartz-alunite rock such as NP1-S5 (Appendix A), formed during the acid sulfate hydrothermal stage of alteration (Stoffregen, 1987; Gray and Coolbaugh, 1994). At Summitville, relict grains of svanbergite-woodhouseite solid solution are included within alunite (Stoffregen and Alpers, 1987, their Fig. 1; this study, samples NP1-S5, ND1, ND3-I, Appendix A). Hinsdalite has been reported in quartz-alunite rock from Summitville (Stoffregen, 1985; Gray and Coolbaugh, 1994), but its exact paragenetic relationship to alunite or to sulfide minerals was not specifically addressed. Lead was derived from galena, which occurs at depth within the vuggy silica zone and in peripheral alteration zones outside of the vuggy silica and quartz- alunite zones (Stoffregen, 1985). In quartz-alunite rock NP1-S5, hinsdalite was only observed with chalcocite and a Cu-sulfate mineral (Fig. 2) in fractures and was not found intergrown with alunite in the interior of the rock. Hinsdalite is abundant in chalcocite-rich samples ND1, ND3-I, and ND3-II. Hinsdalite-rich zones are intergrown with chalcocite, and include relict grains of alunite and solid solutions of alunite and APS minerals, (Figs. 3A, 3B, 4). The textures suggest that hinsdalite formed with the chalcocite, during supergene alteration, and that alunite and APS minerals were replaced at that time. The relationship between hinsdalite and chalcocite is less clear where hinsdalite and late Cu-sulfate minerals form fracture fillings and appear to encrust chalcocite (Fig. 2). Hinsdalite has been reported as a supergene mineral from several localities (Stanley, 1987, and references therein) and as occurring in gossans related to Pb-Zn mineralization in the Mount Isa region, Australia (Scott, 1987). At Summitville, hinsdalite formation serves to remove Pb from the system, at least during supergene alteration and, possibly, during later weathering. The stability and solubility of hinsdalite under different conditions has not apparently been studied experimentally, but such data are desirable to help understand its low-temperature behavior.

SEM-EDS analysis and elemental mapping indicate a range of compositions is represented by the relict grains of alunite and alunite-APS solid solution included in the hinsdalite; but some caution must be applied to this conclusion as some of the grains are small and, in some cases, are probably less than or about the size of the activation volume of the electron beam. Extensive solid solution among members of the alunite-jarosite family is consistent with the results of Scott (1987) and Stoffregen and Alpers (1987).

Hinsdalite-rich zones have been altered to kaolinite + hinsdalite (ND1, Appendix A). During alteration, hinsdalite is apparently preserved and Al, probably at least in part derived from the breakdown of alunite and (or) APS minerals, contributes to the formation of the kaolinite. Aggregates of hinsdalite that are found on rock surfaces (ND3-II, Appendix A) may represent relict grains, rather than precipitates of secondary hinsdalite; the texture is somewhat ambiguous. Hinsdalite that forms aggregates on altered rock surfaces is slightly enriched in Fe and depleted in Al compared to hinsdalite from within the interior of the same rock. This enrichment in Fe may reflect surficial oxidation of the

hinsdalite.

Summitville alunite formed during advanced-argillic alteration, but also occurs as a secondary mineral (SO; Appendix A) with a morphology and, possibly, a composition different from that of the earlier-formed alunite. Stoffregen and Alpers (1987) reported that bladed alunite formed during hydrothermal alteration contained minor amounts of Na. Alunite from quartz-alunite rock NP1-S5 has the habit and Na content, as indicated by SEM-EDS, consistent with the data of Stoffregen and Alpers. Secondary alunite forms pseudocubic grains <5 μm across, texturally similar to secondary jarosite (Fig. 5). Na in secondary alunite is absent or below the detection limit of the SEM-EDS.

Jarosite formed during both pre- and post-mining weathering of the Summitville deposit (Plumlee and others, 1995b). Jarosite has three distinct occurrences in the altered rocks examined in this study that illustrate its development during different stages of alteration. The latest formed jarosite occurs as yellow or orange encrustations (Fig. 5) on altered rock surfaces and along fractures. Jarosite that is disseminated throughout the groundmasses of clay-rich rocks may be the result of either (or both) pre- and post-mining activity. Jarosite also is preserved in relict barite-rich veins. Some jarosite in all three occurrences contains minor P, but no consistent correlation between the presence of P and occurrence was found in this study. The affect of P on the solubility of jarosite has not been reported.

Brown coatings and crusts. Brown crusts (samples TCOSP, MFCOSP, SP-1, SAL-BS) were not identified, but SEM-EDS data indicate that they are a poorly crystalline Fe-sulfate mineral. In plane light, the crusts appear as relatively smooth, uniform coatings, molded on the rock surfaces. In the SEM, no distinct crystal morphology attributed to the coatings was evident. Grains that are coated by the suspected sulfate are evident and SEM-EDS analysis yielded mixed spectra, i.e., peaks attributed to the coated mineral (quartz, kaolinite, etc.) plus $Fe+S\pm P$. Attempts to minimize penetration of the electron beam into the sample (and to maximize the likelihood of only analyzing the coating) by operating at a relatively low accelerating voltage (12-15 kV) did not yield significantly better results. Because the brown crusts are so thin, it was not possible to cleanly separate them from the underlying material. Consequently, XRD analyses yielded mixtures of quartz, clay minerals, and minor jarosite; no other peaks were present in the diffractograms that could be attributed to the crusts.

Na-rich secondary minerals. Sodium-rich secondary minerals, including sideronatrite sodium sulfate, and at least two yet unidentified minerals, form crusts on sample H_2Ot (Appendix A), which was collected downstream from the water treatment plant. The Na compounds that are added to acid mine drainage waters at the treatment plant raise the pH of the drainage waters; these treated waters then react with minerals in the surrounding rocks, producing the Na-bearing secondary minerals.

Fe-rich precipitates of possible bacterial origin

Three compositionally different materials that may be bacterial in origin were observed in the Summitville samples. The morphologies of these materials suggest that they may be the remains of bacteria (E.I. Robbins, USGS, personal communication, 1995) coated by the accumulation of amorphous or poorly crystalline Fe-rich phases, possibly similar to the Fe-rich coatings formed on bacterial cells that were described by Mann and others (1992). The first kind of suspected bacterial material is Fe-rich and forms the stalactite from the Reynolds tunnel (sample AD1500, Appendix A; Fig. 6A-E) and crusts that coat sample surfaces and fractures (samples SO, TCOSP; Appendix A). Two additional possible bacterial materials that are rich in Fe and contain different amounts of

Sb, As, S, and P (sample SO, Appendix 1; Fig 7A, 7B) were also identified. If these materials are bacterial in origin, then their presence at Summitville demonstrates the importance of bacteria in the removal of toxic elements from acid drainage waters. The removal of various elements by bacterial activity has been explored as a remediation method for Summitville spent ore (Thompson and others, 1995).

Reynolds Tunnel stalactite and Fe-rich crusts. Two morphologies are seen in the stalactite and crusts: microspheres, which may be coated bacterial cocci, and rod-shaped forms that may be coated bacilli (Figs. 6A, 6D). All layers of the stalactite are Fe rich, but contain different amounts of S, P, As, Si ,and Al; the different compositions probably reflect changes in water composition over time, as subsequent layers were added. Analogous textural differences in coccus-type morphologies from layered Fe-rich crusts from an area of acid-mine drainage in Virginia have been documented (Flohr, unpub. data). Chapman and others (1983) described a nearly amorphous Fe-rich sediment with a spheroidal texture that was attributed to precipitation of Fe associated with algae; zonation within the sediment was not noted. Fe-rich crusts, which may also be of bacterial origin, consist of microspheres (possible coated cocci) beneath a thin, smooth protective layer (sample SO).

XRD analysis showed that different layers of the stalactite are nearly X-ray amorphous, with only a broad weak maximum at about 2.5 Å apparent in the X-ray patterns. Examination of a split of one XRD powder in the STEM showed that the material consists of round to elongated fragments. The fragments showed no coherent scattering in electron diffraction patterns, but a set of diffuse rings could be easily seen. These rings correspond to the 2.5 Å and 1.5 Å broad maxima of two-line ferrihydrite. (It is also noted that small crystals of magnetite, which were identified by electron diffraction, nucleated easily on edges of the fragments while observing them in the STEM.) Poorly crystalline ferrihydrite that yields two or four broad maxima by XRD is typical of ferrihydrite from areas of mine drainage (e.g., Ferris and others, 1989; Bigham, 1994, and references therein). Dark brown to red-brown goethite was reported from oxidized vuggy silica zones at Summitville (Gray and Coolbaugh, 1994). Poorly crystalline goethite was identified forming a thin crust on sample CW2. The goethite may form as ferrihydrite coarsens with time.

Ferrihydrite has been reported from acidic to alkaline environments (e.g., Ferris and others, 1989; Bigham, 1994). Bigham (1994) suggested that waters with pH>5 and with dissolved Si and (or) high organic matter favored the formation of ferrihydrite over that of jarosite, goethite, schwertmannite, or lepidocrocite. Ferris and others (1989) considered whether the formation of ferrihydrite with a high sulfate content versus a high silica content indicated formation at more or less acidic conditions, respectively. Water sampled from the Reynolds tunnel between October, 1990 and June, 1993 is acidic with pH of 2.7-3.2 and sulfate contents of 1920-4510 mg/L (Plumlee and others, 1995a). These conditions are conducive to the formation of ferrihydrite, as indicated by the formation of the ferrihydrite stalactite (sample AD1500).

Sb- and As-rich materials. It is not known if the Sb- and As-rich materials (sample SO, Appendix A, Figs. 7A, 7B) are precursors of specific minerals. Bowell (1994) referred to an amorphous hydrated ferric arsenate, pitticite, that formed in a lateritic weathering environment, but did not provide additional information about the phase. It is not clear if pitticite is the product of bacterial action and if it is similar to the As-rich material described herein.

Relationship between Secondary Mineralogy and Drainage Chemistry

Several of the samples (CW2, CW3, SAL-BS, and TCOSP) described in this report were the subject of leaching experiments conducted to study element mobility at Summitville (Plumlee and others, 1995a). Some correlations can be made between the abundance of certain elements in leachate water and the presence of water soluble minerals in a given sample. Leachate waters from samples CW2 and CW3 contain high concentrations of SO_4^{2-}, Fe, Al, Cu, Mn, and Zn, which are attributed to the dissolution of the water soluble sulfates halotrichite and melanterite that contain these elements (Appendix A). Dissolution of alunogen also contributes to the high Al concentrations in the leachate waters. Leachate waters derived from sample TCOSP contain moderate amounts of Zn (5.6 ppm) and Cu (18 ppm) (Plumlee and others, 1995a), but no Zn- or Cu-bearing minerals were detected by SEM-EDS. Both elements may occur in secondary minerals in concentrations below the detection limits of the SEM-EDS (at least 500 ppm, depending on the element and on operating conditions). In comparison, leachate waters from sample CW2 contained 120 ppm Zn and semi-quantitative SEM-EDS analysis indicated that some halotrichite and melanterite, which are abundant in CW2, contain up to several wt% ZnO. Some occurrences of the Fe-rich phase that replaced plant material in sample SAL-BS contains minor Cu and is probably the source of the Cu in the sample leachate waters. Drainage and leachate waters were found to contain detectable concentrations of several rare earth elements (REE), Co, Ni, and Cr (Plumlee and others, 1995a). Stoffregen and Alpers (1987) reported Ce in APS minerals from Summitville and traces of an REE-rich phosphate occurs in sample ND2. The sources of the Ni, Fe, and Co in the drainage waters may be relict igneous phases, as was suggested as the source of REE (Plumlee and others, 1995a).

The soluble secondary minerals play a role in the seasonal variation of the composition and acidity of drainage waters (Plumlee and others, 1995a). The soluble sulfate minerals (chalcanthite, alunogen, halotrichite, melanterite, gypsum) form by evaporation or efflorescence during dry periods and are dissolved during wet periods (during the rainy season or periods of snowmelt runoff). When these minerals dissolve, they release metals and acid, contributing to acid mine drainage at the site and to the formation of highly acidic pools.

Brochantite, posnjakite, alunite, and jarosite are classified as relatively less soluble minerals than the soluble sulfates noted above (Alpers and others, 1994). Brochantite and posnjakite do not appear to be as abundant as the readily soluble chalcanthite at Summitville and, so, their formation probably does not contribute to reducing Cu and sulfate in the drainage waters to a large extent. Jarosite is a minor constituent of several samples and is abundant in samples CW2 and CW3. Although alunite is present in a number of the samples examined in this study, it does not appear to be volumetrically significant, with exception of alunite in quartz-alunite rock. Formation of these minerals probably has only relatively minor effect on the compositions of drainage waters.

The formation of relatively insoluble Fe-rich crusts and tentatively identified bacterial materials that contain S, P, As, and Sb, effectively remove these elements from the drainage waters. Fe-rich bacterial floc in drainage areas at Summitville is commonly observed and may also remove the same and (or) other elements from the drainage waters through adsorption. Scorodite is also relatively insoluble and serves as another sink for As and Fe. The formation of hinsdalite through the alteration of galena decreases the availability of Pb to the drainage systems.

CONCLUSIONS

Characterization of secondary minerals that formed as the result of pre-mining weathering and post-mining sulfide oxidation showed that these minerals host a variety of elements, including Cu, Fe, Al, Zn, Mn, As, Sb, Pb, S, and P. Materials that may be bacterial in origin are Fe-rich and contain S, P, As, and (or) Sb. The compositions of the secondary minerals and the suspected bacterial material are dependent, as expected, on the compositions of the earlier-formed (igneous, hydrothermal, supergene) minerals, from which they are derived. Secondary Cu-sulfate minerals form through the oxidation of Cu-sulfides and evaporation of Cu-rich acid-mine drainage waters. Secondary alunite and jarosite form in clay-rich rocks, where K and Al are available. Some of the minerals identified are highly soluble, some are relatively less soluble, and others are relatively insoluble. Halotrichite, alunogen, melanterite (CW2), and chalcanthite (ND2, NP1-S5) are highly soluble and can only form thick crusts during prolonged dry periods or in areas sheltered from precipitation. Highly soluble minerals are, in part, responsible for the seasonal and storm-related increases in metal loads and acidity observed in drainage waters at Summitville (Plumlee and others, 1995a). In arid regions where thick crusts of metal-rich soluble minerals can develop, discharge of metals and acidity into drainage waters during infrequent periods of precipitation can be severe. Insoluble phases effectively remove certain elements from the system. Experimental data that would allow us to better evaluate the solubility of the secondary and supergene minerals, especially those that host potentially toxic elements, are desirable.

For some samples that were the subject of leaching experiments (Plumlee and others, 1995a), it is possible to correlate the concentrations of certain elements in the leachate waters with the presence of certain soluble secondary minerals. For other samples, we can not identify specific minerals that could be the source of high concentrations of elements present in the leachate waters. In the latter case, the concentrations of these elements in the minerals examined may be below the detection limit of the SEM-EDS. Additional analytical work is required to isolate, if possible, and analyze given secondary phases by a more sensitive method. Separation and concentration of the secondary minerals is difficult because of their fine grain size and because they are commonly intimately associated with each other.

Textural characteristics indicate that at least some hinsdalite from Summitville is contemporaneous with the supergene mineral chalcocite. Other textural evidence suggests that hinsdalite may have formed later than chalcocite, consistent with the formation of hinsdalite during different stages of weathering of the deposit. Hinsdalite always occurs with chalcocite and secondary Cu-sulfate minerals in the samples examined. The Cu-sulfates are derived from the oxidation of chalcocite. Textures (e.g., Fig. 2) suggest that in some occurrences hinsdalite and Cu-sulfates are contemporaneous.

Only a small number of samples were examined during this study. It is likely that additional secondary minerals occur at Summitville. Also, given the fine-grained nature of the altered rocks, it is possible that other secondary minerals, present in only minor amounts, were not identified.

ACKNOWLEDGEMENTS

Elaine S. McGee provided helpful advice on SEM sample preparation and analysis methods. Elenora I. Robbins is thanked for informative discussions about bacteria.

REFERENCES CITED

Alpers, C.N., Blowes, D.W., Nordstrom, D.K., and Jambor, J.L., 1994, Secondary minerals and acid mine-water chemistry: *in* Jambor, J.L. and Blowes, D.W., eds., Environmental geochemistry of sulfide mine-wastes, Mineralogical Association of Canada, p. 247-270.

Bigham, J.M., 1994, Mineralogy of ochre deposits formed by sulfide oxidation: *in* Jambor, J.L. and Blowes, D.W., eds., Environmental geochemistry of sulfide mine-wastes, Mineralogical Association of Canada, p. 103-132.

Bowell, R.J., 1994, Sorption of arsenic by iron oxides and oxyhydroxides in soils: Applied Geochemistry, v. 9, p. 279-286.

Chapman, B.M., Jones, D.R., and Jung, R.F., 1983, Processes controlling metal ion attenuation in acid mine drainage systems: Geochimica et Cosmochimica Acta, v. 47, p. 1957-1973.

Ferris, F.G, Tazaki, K., and Fyfe, W.S., 1989, Iron oxides in acid mine drainage environments and their association with bacteria: Chemical Geology, v. 74, p. 321-330.

Flohr, M.J.K., Dillenburg, R.G., and Plumlee, G.S., 1995, Characterization of secondary minerals formed as the result of weathering of the Anakeesta Formation, Alum Cave, Great Smoky Mountains National Park, Tennessee: U.S. Geological Survey Open-file Report 95-477, 22 p.

Gray, J.E., and Coolbaugh, M.F., 1994, Geology and geochemistry of Summitville, Colorado: An epithermal acid sulfate deposit in a volcanic dome: Economic Geology, v. 89, p. 1906-1923.

Gray, J.E., Coolbaugh, M.F., and Plumlee, G.S., 1993, Geologic Framework and environmental geology of the Summitville, Colorado acid-sulfate mineral deposit: U.S. Geological Survey Open-file Report 93-677, 29 p.

Gray, J.E., Coolbaugh, M.F., and Plumlee, G.S., 1994, Environmental geology of the Summitville mine, Colorado: Economic Geology, v. 89, p. 2006-2014.

Jambor, J.L., 1994, Mineralogy of sulfide-rich tailings and their oxidation products: *in* Jambor, J.L. and Blowes, D.W., eds., Environmental geochemistry of sulfide mine-wastes, Mineralogical Association of Canada, p. 59-102.

Mann, H., Tazaki, K., Fyfe, W.S., and Kerrich, R., 1992, Microbial accumulation of iron and manganese in different aquatic environments: An electron optical study: *in* Skinner, H.C.W. and Fitzpatrick, R.W., eds., Biomineralization processes of iron and manganese: modern and ancient environments, Catena, p. 115-131.

Patton, H.B., 1917, Geology and ore deposits of the Platoro-Summitville mining district, Colorado: Colorado Geological Survey Bulletin 13, 122 p.

Plumlee, G.S., and Edelman, P., 1995, An update on USGS studies of the Summitville mine and its downstream environmental effects: U.S. Geological Survey Open-file Report 95-23, 9 p.

Plumlee, G.S., Smith, K.S., Mosier, E.L., Ficklin, W.H., Briggs, P., and Meier, A., 1995a, Geochemical processes controlling acid-drainage generation and cyanide degradation at Summitville: *in* Posey, H.H., Pendleton, J.A., and Van Zyl, D., eds. Proceedings: Summitville Forum '95, Colorado Geological Survey Special Publication 38, p. 23-34.

Plumlee, G.S., Gray, J.E., Roeber, M.M., Jr., Coolbaugh, M., Flohr, M., and Whitney, G., 1995b, The importance of geology in understanding and remediating environmental problems at Summitville: *in* Posey, H.H., Pendleton, J.A., and Van Zyl, D., eds. Proceedings: Summitville Forum '95, Colorado Geological Survey Special Publication 38, p. 13-22.

Princeton Gamma-Tech, Inc., 1994, Integrated microanalyzer for imaging and X-ray software manual, v. 7. Princeton, N.J.

Scott, K.M., 1987, Solid solution in, and classification of, gossan-derived members of the alunite-jarosite family, northwest Queensland, Australia: American Mineralogist, v. 72, p. 178-187.

Stanley, C.R., 1987, Hinsdalite and other products of oxidation at the Daisy Creek stratabound copper-silver prospect, northwestern Montana: Canadian Mineralogist, v. 25, p. 213-220.

Stoffregen, R.E., 1985, Genesis of acid-sulfate alteration and Au-Cu-Ag mineralization at Summitville, Colorado: Unpublished Ph.D. dissertation, Berkeley, University of California, 205 p.

Stoffregen, R., 1987, Genesis of acid-sulfate alteration and Au-Cu-Ag mineralization at Summitville, Colorado: Economic Geology, v. 82, 1575-1591.

Stoffregen, R.E. and Alpers, C.N., 1987, Woodhouseite and svanbergite in hydrothermal ore deposits: Products of apatite destruction during advanced argillic alteration: The Canadian Mineralogist, v. 25, p. 201-211.

Thompson, L., Steiner, J., and Whitney, G., 1995, Biomineralization of Summitville spent ore: SEM investigation of biomineralized metallic films, *in* Posey, H.H., Pendleton, J.A., and Van Zyl, D., eds. Proceedings: Summitville Forum '95, Colorado Geological Survey Special Publication 38, p. 152-158.

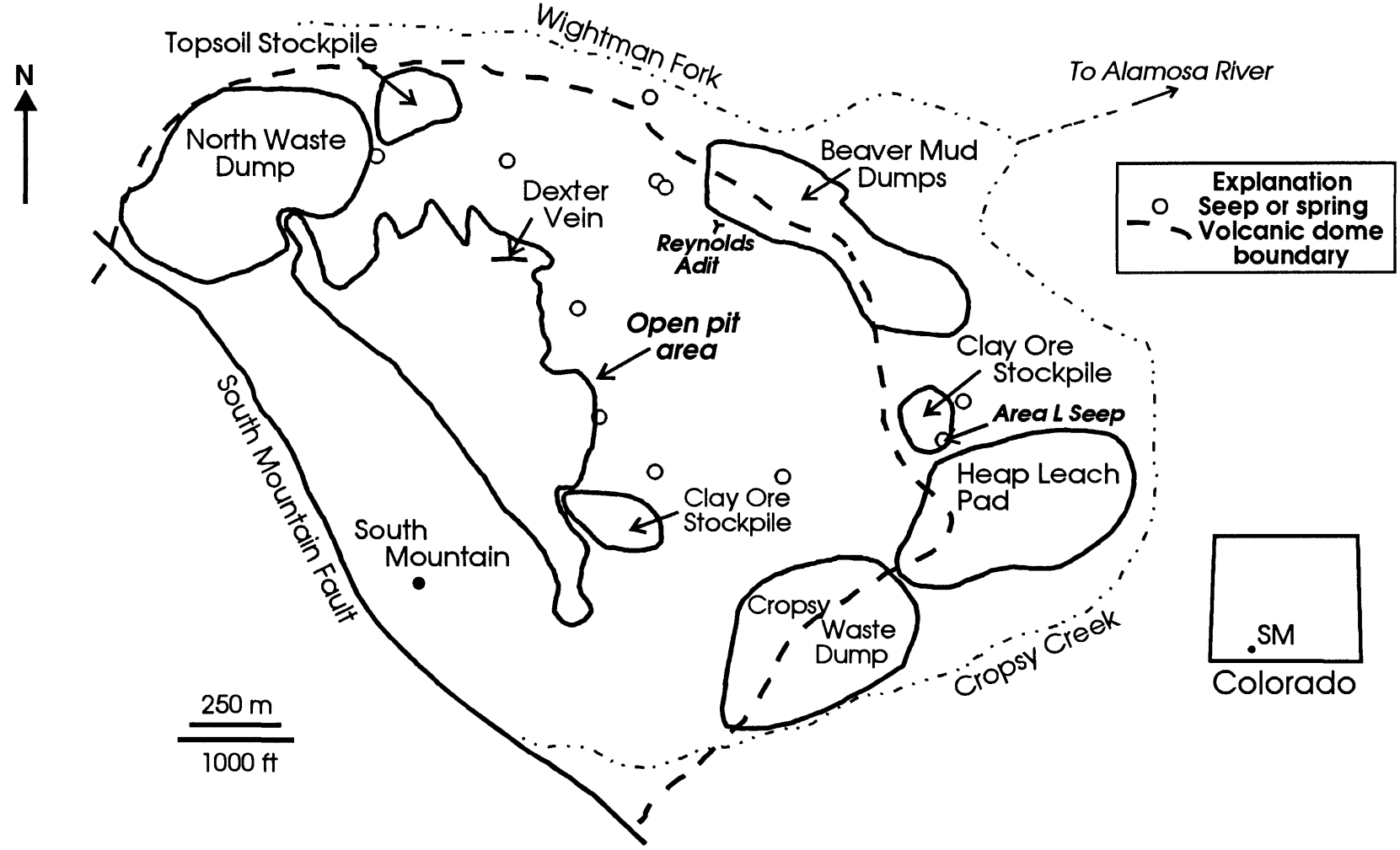

Figure 1. Highly simplified map of the Summitville mine site (SM on the state index map) showing the location of several mine waste dumps and seeps (after Plumlee and others, 1995b).

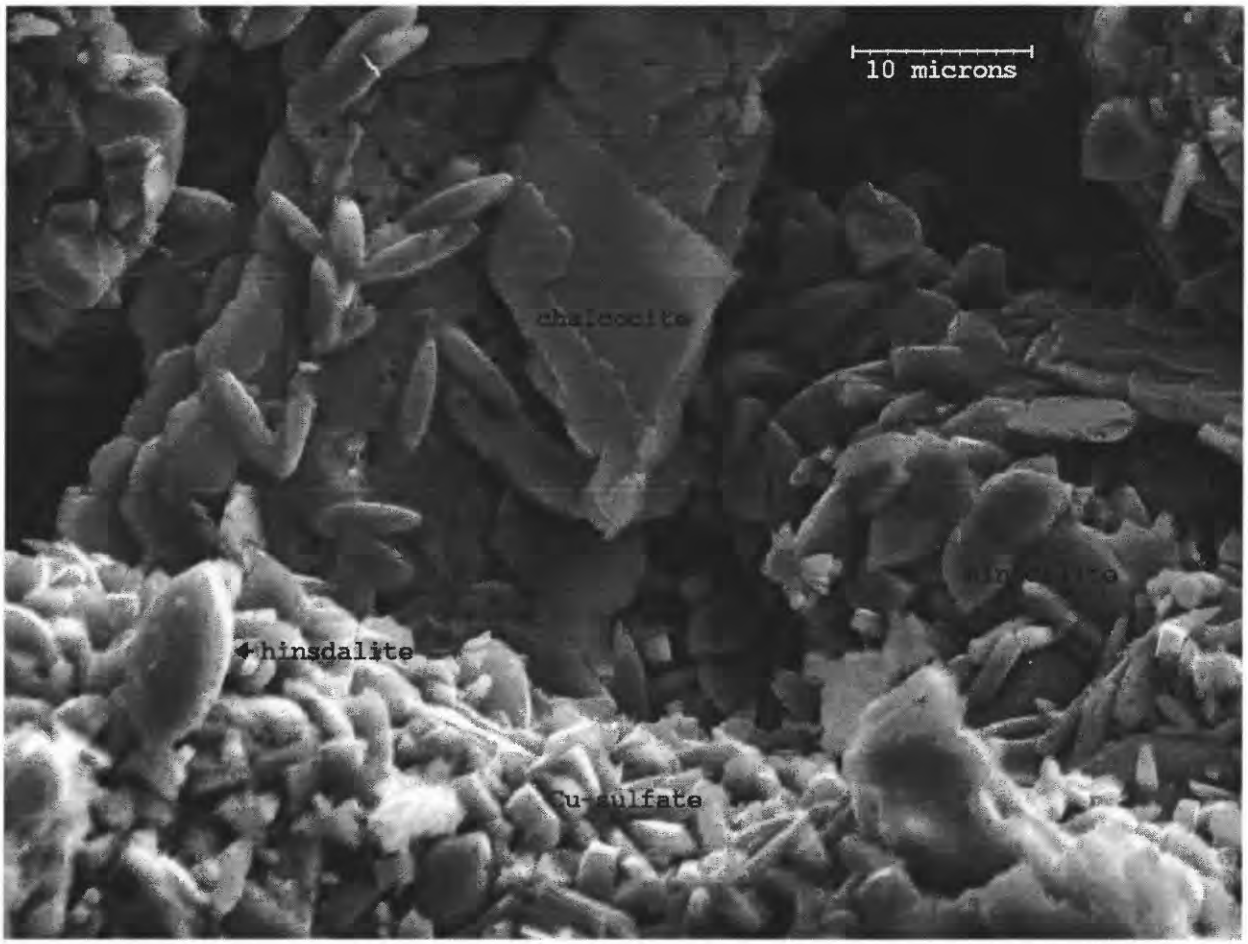

Figure 2. Aggregates of hinsdalite and a Cu-sulfate mineral that encrust partly altered plates of chalcocite from a fracture in quartz-alunite rock NP1-S5. The texture seen here suggests that the hinsdalite may have formed after chalcocite, rather than contemporaneously with chalcocite as a supergene mineral, as suggested by the textures seen in Figures 3A, 3B, and 4. (Secondary electron image)

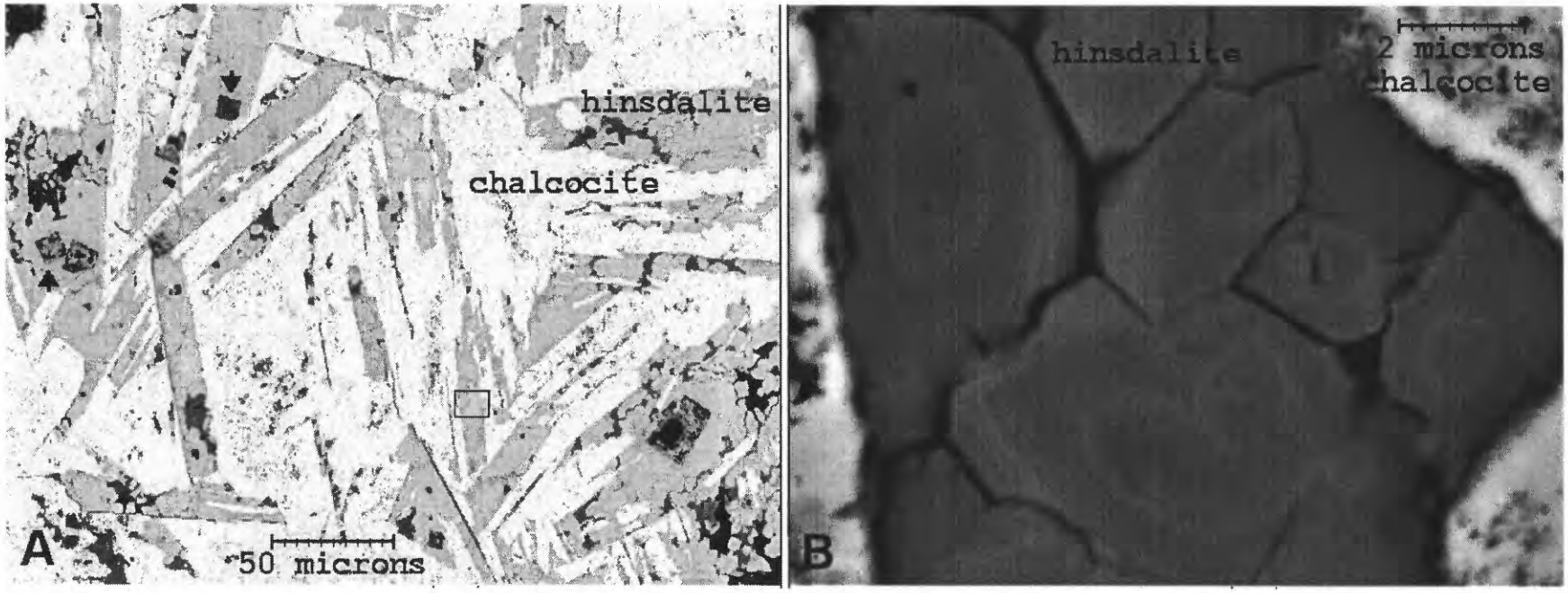

Figure 3. Chalcocite-hinsdalite intergrowths. (A) "Laths" of hinsdalite include euhedral grains with compositions in the range of alunite-APS solid solution (dark grains with square cross-sections; examples at arrows, upper left quadrant). The lath-like morphology suggests that hinsdalite has replaced laths of alunite that originally included the relict pseudocubic grains (see Stoffregen and Alpers, 1987, their Fig. 1 for comparison). The "laths" are now composed of minute grains of hinsdalite, as seen in (B). The area shown in (B) is indicated by the boxed area. (B) Finely zoned grains of hinsdalite that form the "laths" seen in (A). (Back-scattered electron images; sample ND3-I)

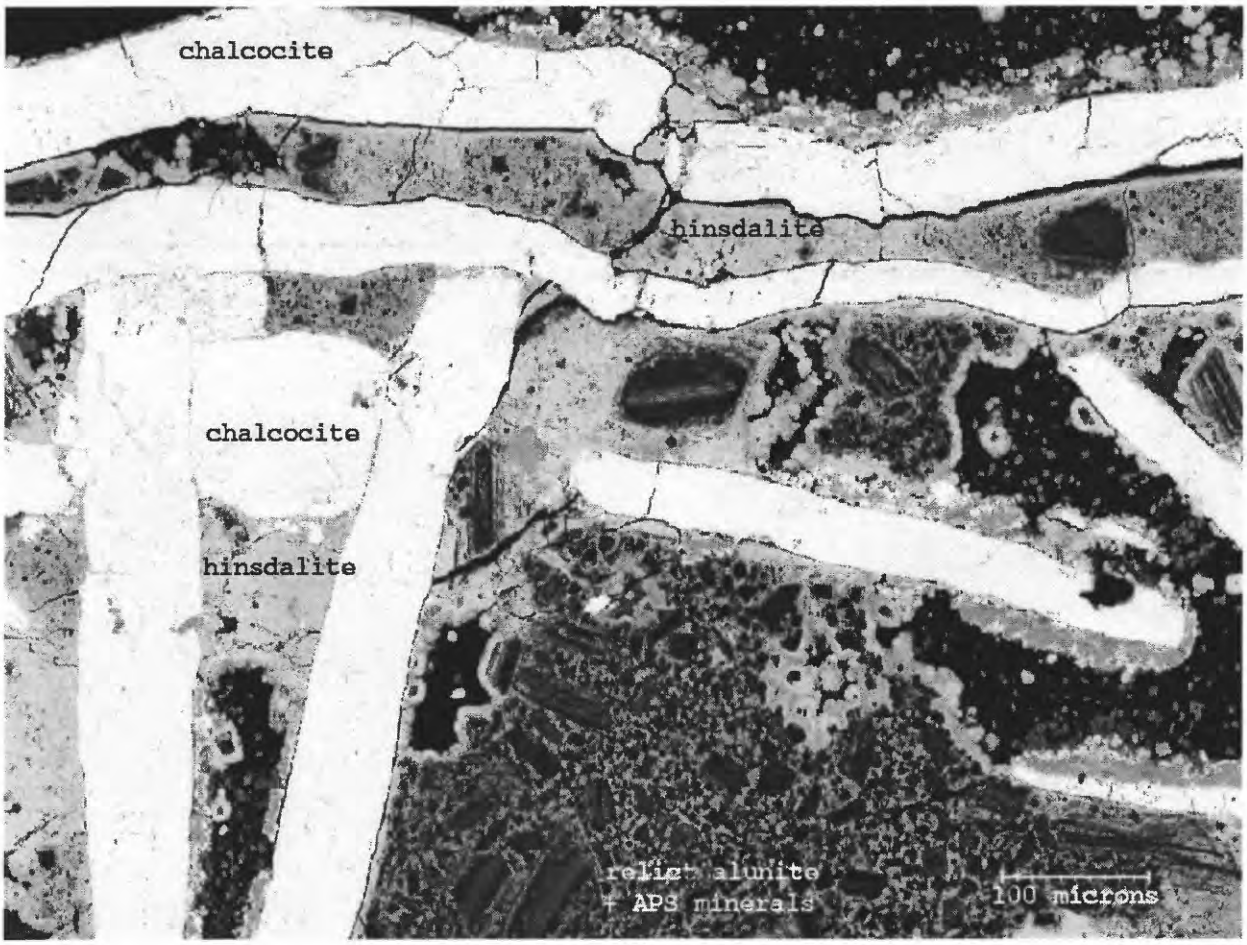

Figure 4. Intergrowths of chalcocite plates (brightest white areas) and hinsdalite (medium gray areas) that surround relict grains of alunite (large, dark tabular grains) and aluminous phosphate-sulfate (APS; dark grains associated with alunite) minerals, including grains with compositions consistent with alunite-APS solid solution. Note that hinsdalite is always in contact with the chalcocite; relict alunite and APS grains were never observed in contact with chalcocite. In other parts of the same polished section, relict alunite and APS minerals are less abundant and hinsdalite is more abundant than seen here. Black areas are vugs in the sample. (Back-scattered electron image; sample ND1)

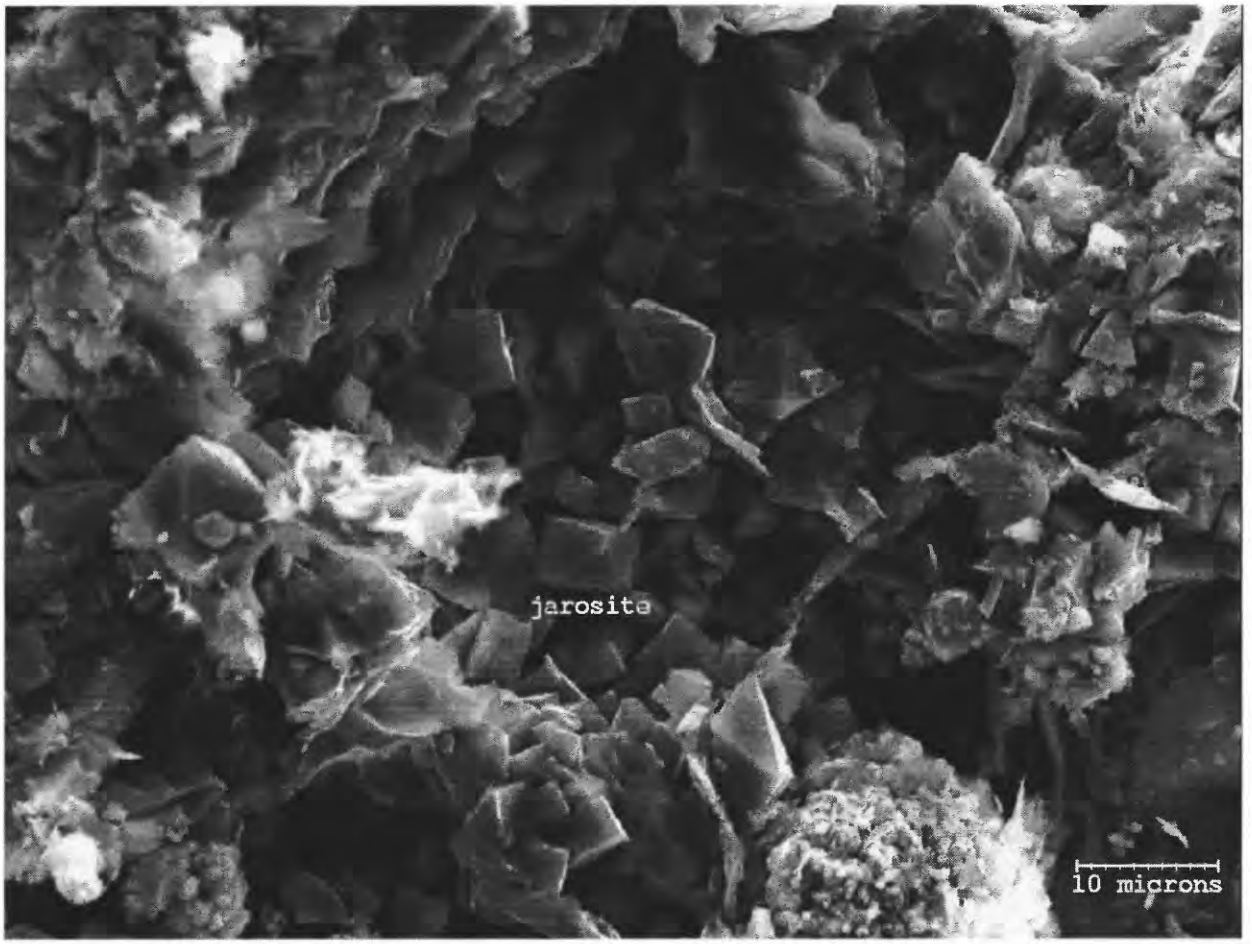

Figure 5. Jarosite that forms a yellow crust on sample CW3. This euhedral crystal form and grain size are typical of jarosite and, also, of late-stage alunite from the Summitville samples examined in this study. The surrounding grains are clay minerals. (Secondary electron image)

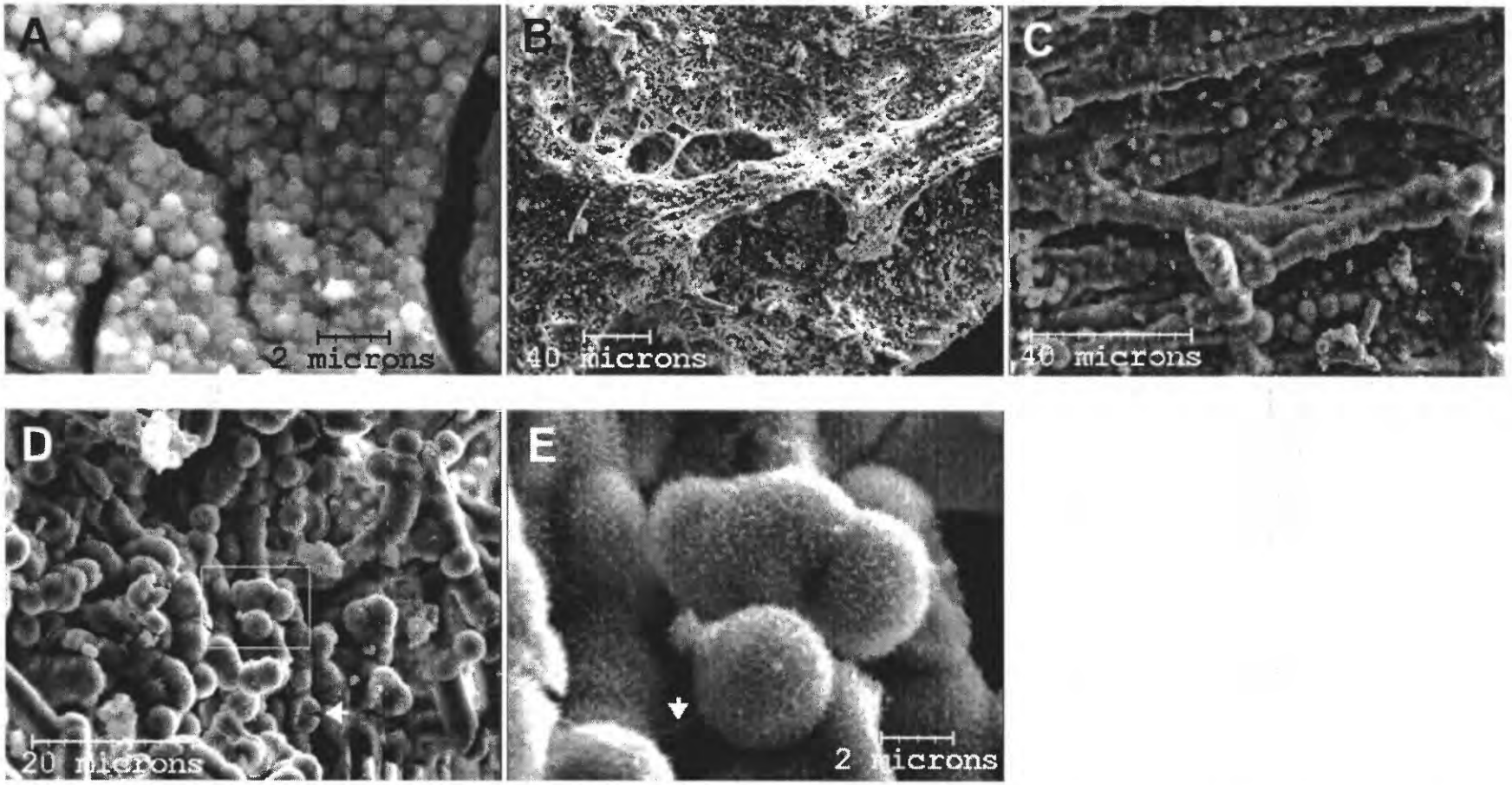

Figure 6. Examples of bacterial-type textures observed in stalactite AD-1500 from the Reynolds adit. (A) The outer surface of the stalactite is composed of submicron microspheres with relatively smooth surfaces. (B) The inner surface of the fragment shown in (A) is composed of filamentous structures, shown in detail in (C), that form a porous network. (C) The filamentous structures are composed of string-like microspheres and have a spongy or "fuzzy" appearance. (D) In some interior layers of the stalactite, microspheres and rod-shaped bodies form aggregates. Note the broken microsphere (at arrow, lower center of image), with a smooth inner surface, similar to the surfaces of the microspheres that form the outer layer of the stalactite [seen in (A)], and a spongy outer surface; the layering of this sphere illustrates progressive development. The development of the microspheres that form the outer layer of the stalactite was arrested when the stalactite was collected and removed from its environment of formation, before sheath material developed around the individual cells. The box in the center of the field of view marks the area shown in (E). (Note that the streaking in the lower right of the image is due to charging of the sample under the electron beam.) (E) High magnification image of spongy microspheres (D) shows the detailed texture of the surfaces and a fine "thread," possibly a slime connection (at arrow), typical of those commonly observed connecting neighboring microspheres.

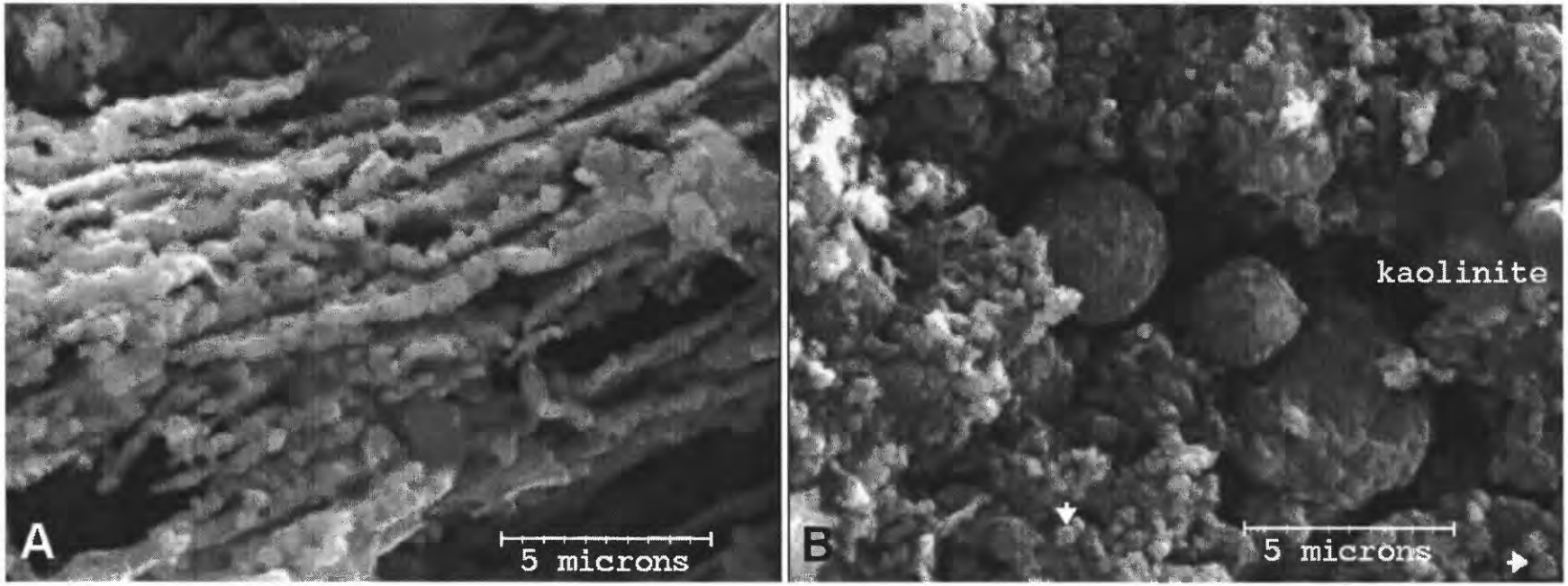

Figure 7. Examples of bacterial-type materials. (A) Bright yellow material that coats exposed surfaces of covellite grains in sulfide-mineralized vuggy quartz rock (sample SO). The material is made up of submicron-sized microspheres, strung together to form chains or filaments. SEM-EDS analysis showed that this material is rich in Fe and Sb, with minor As and S. The host rock contains pyrite and Sb-bearing enargite, sources of the elements found in the yellow material. (B) Tan material found in vugs in the same sample, SO, as the yellow material shown in (A). Here, the tan material consists of aggregates of micron-to-submicron-sized material, including microspheres (examples of small spheres at arrows, lower right and near bottom center) and larger individual spheres (two spherical bodies in the center of the field of view). The microspheres may be bacterial in origin and the larger spheres are more in the size range of algae (E. I. Robbins, USGS, personal communication, 1995). SEM-EDS analysis showed that this material is rich in Fe and As, with minor Sb and S. (Secondary electron images)

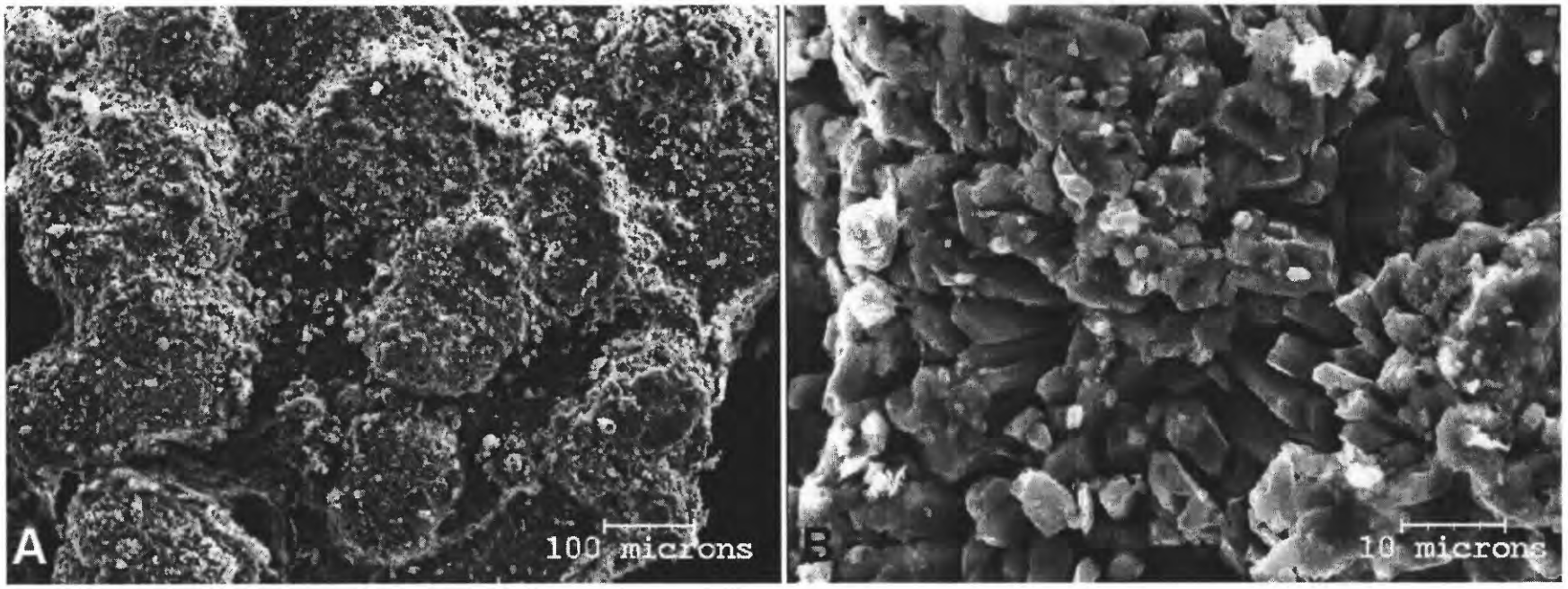

Figure 8. (A) Nodular gypsum-rich crust on clay-rich sample MFCOSP. (B) Rosettes of radiating gypsum laths form the nodules. (Secondary electron images)

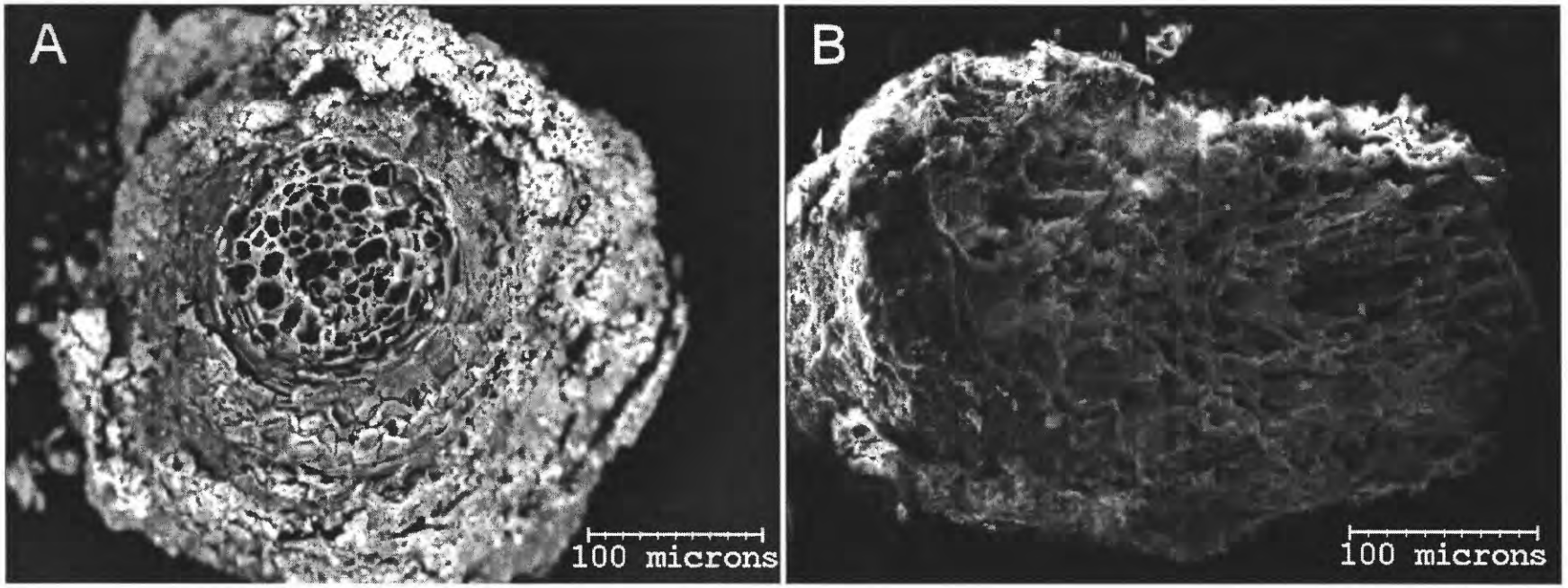

Figure 9. (A) Cross-section of replaced plant material, typical of a stem or twig, having porous cellular structure in the core, surrounded by a zone, which shows growth rings, of compressed cells. Outer zone of adhering material is from the clay-rich rock matrix. SEM-EDS indicates that the plant fragment was replaced by an Fe- and S-rich phase, with minor P. (Back-scattered electron image; sample SAL-BS) (B). Longitudinal view of a preserved plant fragment, possibly a stem or twig, encrusted by adhering clay (on the left side). SEM-EDS indicates that this fragment is compositionally similar to the fragment in (A). (Secondary electron image; sample SAL-BS)

Table 1. Ideal chemical formulas of minerals identified in this study, Summitville mine site

Mineral	Ideal formula
Relict igneous	
alkali feldspar	$(K,Na)AlSi_3O_8$
plagioclase feldspars (albite-anorthite ss)	$NaAlSi_3O_8$ - $CaAl_2Si_2O_8$
TiO_2 polymorphs (anatase, rutile)	TiO_2
zircon	$ZrSiO_4$
chlorapatite	$Ca_5(PO_4)_3Cl$
Formed during argillic alteration	
quartz	SiO_2
kaolinite	$Al_2Si_2O_5(OH)_4$
illite	$K(Al,Mg,Fe)_2(Si,Al)_4O_{10}(OH)_2$
chlorite	$(Mg,Fe,Al)_{12}(Si,Al)_8O_{20}(OH)_{16}$
alunite[1]	$KAl_3(SO_4)_2(OH)_6$
woodhouseite-svanbergite ss[1]	$(Ca,Sr)Al_3(PO_4)(SO_4)(OH)_6$
pyrite	FeS_2
Hydrothermal/supergene	
enargite	Cu_3AsS_4
sphalerite	ZnS
covellite	CuS
chalcocite	Cu_2S
barite	$BaSO_4$
hinsdalite[1]	$(Pb,Sr)Al_3(PO_4)(SO_4)(OH)_6$
Pre-mining secondary	
sulfate minerals	
jarosite[1]	$KFe_3(SO_4)_2(OH)_6$
alunite[1,2]	$KAl_3(SO_4)_2(OH)_6$
Fe-oxides and hydroxides	
goethite	$FeO(OH)$
ferrihydrite	$2.5Fe_2O_3 \cdot 4.5H_2O$
arsenate mineral	
scorodite	$FeAsO_4 \cdot H_2O$
Post-mining secondary	
sulfate and sulfate-phosphate minerals	
jarosite[1]	$KFe_3(SO_4)_2(OH)_6$
alunite[1,2]	$KAl_3(SO_4)_2(OH)_6$
chalcanthite	$Cu(SO_4) \cdot 5H_2O$
brochantite	$Cu(SO_4)(OH)_6$
posnjakite	$Cu_4(SO_4)(OH)_6 \cdot H_2O$
gypsum	$Ca(SO_4) \cdot 2H_2O$
halotrichite	$FeAl_2(SO_4)_4 \cdot 22H_2O$
alunogen	$Al_2(SO_4)_3 \cdot 17H_2O$
melanterite	$Fe(SO_4) \cdot 7H_2O$
sodium sulfate	$NaSO_4$
sideronatrite	$NaFe(SO_4)_2(OH) \cdot 3H_2O$
hinsdalite[1,3]	$(Pb,Sr)Al_3(PO_4)(SO_4)(OH)_6$

[1] members of the alunite-jarosite group; [2] alunite occurs as a secondary mineral, but whether it formed as the result of pre-mining weathering or post-mining is not clear; [3] identification as a secondary mineral is tentative, based on occurrence with Cu-sulfate in fracture fillings (Fig. 2); it is not clear to which group of secondary minerals hinsdalite belongs in this occurrence.
ss = solid solution.

Table 2. Mineralogy of samples from the Summitville mine site [+ = mineral present; ? = tentative identification based on XRD and (or) SEM-EDS data]

Rock type	Altered sulfide-rich rocks			Vuggy quartz	Quartz-alunite	Altered clay-rich rocks			
Sample	ND1	ND3-I	ND3-II	SO	NP1-S5	TCOSP	MFCOSP	CW2	CW3
Mineral									
Relict igneous									
alkali feldspar		+				+	+	+	+
plagioclase feldspar			+						
TiO_2 polymorph		+	+	+	+		+		+
biotite						+	+		
zircon							+		
Argillic alteration									
quartz		+	+[1]	+[1]	+[1]	+[1]	+	+	+
kaolinite	+	+	+		+	+	+	+	+
illite		+			+	+	+	+	
montmorillonite						+			
alunite		+			+	+	+		
woodhouseite-svanbergite ss					+	+	+		
alunite-APS ss[2]	+	+							
pyrite[3]	+	+	+	+	+	+	+	+	+
Hydrothermal/ supergene									
enargite	+	+	+	+	+				
sphalerite		+							
covellite				+					
chalcocite	+	+	+	+	+				
barite		+							
hinsdalite		+	+		+				
Secondary[4]									
jarosite	+		+	+	+	+	+	+	
alunite			+		?	?			
hinsdalite[5]	+		+		+				
scorodite				+					
chalcanthite					+				
brochantite		+							
posnjakite		+							
Cu-sulfate(s) (unidentified)	+				+				
gypsum	+				+	+	+	+	+
halotrichite								+	+
alunogen								+	+
melanterite								+	+
goethite					+	+		+	+
Fe-rich crust		+		+	+	+			
Fe-Sb bacterial(?) material				+					
Fe-As bacterial(?) material				+					

Table 2. Mineralogy of samples from the Summitville mine site (continued)

Rock type	Altered clay-rich rocks					Stalactite
Sample	NDP	ND2	SP1	SAL-BS	H_2Ot	AD1500
Mineral						
Relict igneous						
alkali feldspar	?	+		+	+	
plagioclase	+			+		
TiO_2 polymorph	+	+	+	+		
apatite		+				
REE-phosphate		?				
biotite	+			+		
zircon	+					
Argillic alteration						
quartz	+[1]	+	+	+[1]	+	
kaolinite	+	+	+	+	+	
illite	+	+	+	+	+	
montmorillonite/ smectite			?	+		
chlorite	+					
sericite	+					
alunite	+		+	?		
woodhouseite-svanbergite ss		+	+	+		
alunite-APS ss[2]	+					
pyrite	+	+	+	+	+	
Hydrothermal/ supergene						
enargite		?				
hinsdalite		?				
barite				+		
Secondary[4]						
jarosite	+		+	+	+	
alunite	+					
hinsdalite[5]	+					
chalcanthite		+				
Fe-sulfate(s)	+			+		
sodium sulfate					+	
sideronatrite					?	
Na-sulfates (unidentified)					+	
Fe-arsenate				+		
goethite	+				+	
Fe-rich crust	+			+		
ferrihydrite						+

[1] in these samples drusy quartz that formed during hydrothermal alteration was also found;
[2] aluminous phosphate-sulfate minerals with a range of compositions indicating alunite-woodhouseite-svanbergite solid solution, with other elements present in minor amounts (see descriptions in Appendix A);
[3] no attempt was made to distinguish between pyrite that formed during argillic alteration and that which formed during hydrothermal alteration;
[4] includes pre-mining and post-mining secondary minerals (Table 1) - see sample descriptions (Appendix 1) and text for discussions of secondary phases in individual samples;
[5] identification of hinsdalite as a secondary phase is tentative.

Appendix A. Descriptions of altered rocks, Summitville mine

Sulfide-rich rocks

N. Dexter 1 (ND1): Chalcocite, pyrite, hinsdalite, and enargite form the bulk rock. The outer part of the rock consists of thin curved plates of chalcocite that are interlaminated with pink-tan hinsdalite-rich zones. Relict grains of alunite and APS minerals are preserved within the unaltered interior parts of the hinsdalite-rich zones (Fig. 4). In the outer altered zone of the rock, the hinsdalite zones are altered to a mixture of hinsdalite + kaolinite. Kaolinite, which forms a thin layer on the altered hinsdalite + kaolinite zones, gypsum, and aggregates of subhedral-to-euhedral hinsdalite are found on the rock surface. Unidentified Cu-sulfate minerals (green to blue-green) form thin efflorescent crusts on kaolinite and chalcocite.

N. Dexter 3-I (ND3-I): Enargite, chalcocite, and pyrite form the bulk rock. The interior of the rock is dense and appears relatively unaltered, although hinsdalite and the Cu-sulfate minerals brochantite and posnjakite are developed along fractures. Relict grains of sphalerite, with sparse euhedral barite inclusions, and enargite occur within chalcocite and are altered along fractures and grain margins. An intermediate zone consists of chalcocite + hinsdalite. In part, this zone is texturally similar to sample ND1, with chalcocite plates intergrown with hinsdalite-rich zones. In other parts of the intermediate zone, masses of hinsdalite grains form "laths" that are intergrown with chalcocite and that are tentatively identified as pseudomorphs after alunite (Fig. 3A); this texture may represent a more advanced replacement of alunite by hinsdalite than observed in parts of sample ND1. Pseudocubic grains (most plucked during polishing) within these hinsdalite "laths" are relict APS minerals with compositions in the svanbergite-woodhouseite-alunite solid solution series, as indicated by the presence of Sr, Ca, and K. Hinsdalite grains are usually $< 10\ \mu m$ across, euhedral to subhedral, and are compositionally zoned (Fig. 3B) with slightly higher Fe in the rims. Because the hinsdalite grains are so small and finely zoned, it is difficult to better characterize the compositional differences among the zones (the activation volume of the electron beam probably exceeds the thicknesses of individual zones). The outer part of the rock is altered and is partly covered by a yellow coating that is a fine-grained mixture of kaolinite, quartz, illite, hinsdalite, fragments of the sulfide minerals, a TiO_2 polymorph, and tentatively identified jarosite. One surface of the rock is partly coated with a red-brown crust that consists of an Fe-rich mineral, probably an oxyhydroxide, and aggregates of hinsdalite grains.

N. Dexter 3-II (ND3-II): Sulfide-mineralized vuggy quartz rock with enargite, pyrite, and chalcocite. Grains of a TiO_2 polymorph and the sulfide minerals are intergrown with quartz. A sulfide-rich zone consists of enargite, minor chalcocite, and aggregates of hinsdalite. An unidentified Cu-sulfide mineral that contains minor Sn, as identified by SEM-EDS, is intergrown with the enargite. The Sn-bearing mineral is uncommon and forms lath-like to needle-like grains. The presence of a Sn-bearing phase is surprising as Sn has not been reported from the mine site, although Sn was also detected in one of the suspected bacterial material in sample SO, described below. Element mapping with the SEM showed that chalcocite is altered along fractures: zones that are depleted in Cu and enriched in S relative to the unaltered parts of the grains have developed. The enargite is partly oxidized and is coated with fine-grained blue to green-blue Cu-sulfate minerals, including brochantite and posnjakite. The altered surface of the quartz-rich part of the rock consists of kaolinite with disseminated sulfide minerals and (or) hinsdalite. Patches of a tan-pink coating are similar to the altered hinsdalite-rich zones in sample ND1 and consist of kaolinite with disseminated hinsdalite. Blue to blue-green efflorescences of Cu-sulfate minerals formed on the kaolinite-

rich coatings. Relict albite grains, with extensive dissolution textures, are preserved in the kaolinite.

Summitville Ore (SO): Sulfide-mineralized vuggy quartz rock with successive secondary coatings. Sulfide minerals include covellite, enargite (which is zoned with respect to As and Sb), and pyrite. Anatase is an accessory phase and is intergrown with quartz. Surfaces of pyrite grains show a range of dissolution textures, from slight to extensive. Enargite is surficially altered to a black sooty phase. Scorodite is an uncommon secondary phase.

Evidence for possible bacterial activity: Covellite that is exposed on the outer surfaces of the rock is partly coated with a bright yellow material that is X-ray amorphous and may be a product of bacterial activity. It is composed of what are tentatively identified as filaments of cocci that form short chains (Fig. 7A). SEM-EDS indicates that the material is rich in Fe and Sb, with accessory As and S. There is some variation in composition from area to area. Examination with the SEM showed that soft tan material extracted from vugs and from areas beneath the red crust (described below) may also be bacterial in origin: the material consists of rod-shaped structures that may be bacillus, smooth and spongy-textured microspheres that may be cocci in the size range of < 1 μm to 3 μm in diameter (Fig. 7B), and filamentous-type structures that are chains of spherical bodies, texturally similar to those observed in the yellow material. Aggregates of submicron-sized particles are also present. The tan material is rich in Fe and contains As, S, Sb, and, in some occurrences, a trace of P. The composition of the tan material is not consistent from area to area and, in one unusual occurrence, minor amounts of Sn were detected (see description of ND3-II, above, for comments on the occurrence of Sn).

Red to red-brown crusts: The surface of the rock is coated with a dark red to red-brown crust. Based on one broad, weak peak at about 2.53Å, the crust is tentatively identified as one-line ferrihydrite (see text for discussion and the description of sample AD-1500 in this appendix). Different textures and compositions were found in different parts of the crust. All areas of the crust are rich in Fe, but contain different amounts of S, As, and Sb. Textures range from smooth, to spongy, to smooth with a "swiss-cheese-like" dissolution texture.

Alteration zone between the Fe-rich crust and the quartz-rich rock: A thin zone of soft material with a range of colors (tan, tan-pink, yellow, orange) occurs between the Fe-rich crust and the bulk of the rock. Alunite, jarosite, and minerals with intermediate compositions comprise this zone; alunite appears to be the most abundant of these minerals. The minerals all exhibit the pseudocubic morphology that is typical of secondary alunite and jarosite and all grains are < 5 μm, and more typically < 3 μm, across. Minor amounts of Pb and P were found in some occurrences.

Coatings on Fe-rich crust: The Fe-rich crust is partly coated by thin layers of minerals of the alunite-jarosite group, some of which have a significant hinsdalite component as indicated by the presence of Pb and P. SEM examination showed that the coatings are composed of aggregates of grains that are less than a few microns across.

N. Pit 1 - Solid 5 (NP1-S5): Quartz-alunite rock with sulfide-rich zone that forms one surface of the rock. Alunite contains relict grains, < 20 μm across, of woodhouseite-svanbergite solid solution, with minor Ba + K. A TiO_2 polymorph, pyrite, and enargite are accessory minerals in the quartz-alunite rock. Chalcanthite and kaolinite with accessory gypsum encrust surfaces of the quartz-alunite part of the rock. The sulfide-rich zone consists of abundant enargite and chalcocite. A Cu-sulfate mineral and hinsdalite encrust chalcocite along fractures (Fig. 2). Orange jarosite partly coats kaolinite- and sulfide-rich surfaces. A rare unidentified waxy green mineral, tentatively identified as a Cu-sulfate mineral, based on

SEM-EDS, forms a thin coating on kaolinite in isolated occurrences.

Clay-rich rocks

Top of the Clay Ore Stock-Pile (TCOSP): Mineral clasts in a clay-rich matrix. Part of the sample surface is covered by a brown coating, tentatively identified as an Fe-sulfate (see text for discussion). Grains and aggregates of quartz, albite, K-feldspar, pyrite, goethite, alunite, APS minerals (woodhouseite-svanbergite solid solution) TiO_2 polymorph, and Ti-bearing biotite, are embedded in an illite-kaolinite-rich groundmass. Jarosite is finely disseminated throughout the rock. Alunite occurs as tabular grains that are found throughout the clay-rich groundmass, and is interpreted as a relict, rather than a secondary, phase. Veins of orange jarosite, dark red-brown goethite, and euhedral barite are preserved. Gypsum and jarosite form secondary encrustations. In a clast of drusy quartz, quartz crystals are partly coated by orange-brown Fe-rich microspheres that contain minor P and S and may be bacterial in origin.

Mudflats - Clay ore Stock Pile (MFCOSP) Dense coherent clay-rich rock with a finely nodular surface. Grains and aggregates of quartz, K-feldspar, albite, Ti-bearing biotite, pyrite, goethite, alunite, a TiO_2 polymorph, zircon, APS minerals (woodhouseite-svanbergite solid solution) are embedded in a clay-rich groundmass of illite and kaolinite. Radiating rosettes of gypsum laths form the nodules on the surface (Figs. 8A, 8B) and are partly covered by a thin brown coating, similar to that found in sample TCOSP. Grains of jarosite are finely disseminated in the clay groundmass.

Cropsy Wall 2 (CW2): Extremely altered porous rock with quartz, pyrite, K-feldspar, kaolinite, illite and abundant development of secondary sulfate minerals that form thick efflorescent crusts. The sulfate minerals identified are jarosite, halotrichite, melanterite, alunogen, and gypsum. Jarosite forms pseudocubic grains, $<10\ \mu m$ across (and, more commonly, 1-2 μm across), and appears concentrated in soft yellow zones along fractures within the rock. SEM-EDS indicates that jarosite contains minor Al and P. Halotrichite occurs as (1) white to nearly colorless aggregates of fine needles, (2) tan to pink nodular encrustations, (3) pale yellow nodular encrustations, and (4) medium pink-orange to pink aggregates of needles or nodular encrustations. The color of the halotrichite reflects the presence of different amounts of Mg, Mn, Zn, and Cu, which substitute for Fe. White to nearly colorless halotrichite consistently contains the least amount of minor elements, whereas the more highly colored halotrichite apparently contains a range of concentrations of the aforementioned elements, with more intensely colored occurrences containing highest concentrations. The nodular halotrichite consists of relatively dense aggregates of needles; individual needles can exceed $100\mu m$ in length. Alunogen forms white to cream encrustations. Aggregates of melanterite crystals, which contain minor Mn, Cu, and Zn, are intergrown with alunogen plates and form efflorescences on halotrichite. Individual melanterite grains are $< 5\mu m$ across. Gypsum is uncommon and forms euhedral grains, up to $100\mu m$ long, associated with halotrichite. Halotrichite and alunogen form somewhat botryoidal crusts on the rock and are developed within the rock along fractures. Parts of the rock are quite porous and have been extensively replaced by the secondary sulfate minerals.

Cropsy Wall 3 (CW3): The mineralogy of sample CW3 is, overall, like that described for sample CW2 above. CW3 differs from CW2 in the following respects. The rock is not as porous and the efflorescent minerals are not as thickly developed as in sample CW2. Jarosite, however, is more abundant and is more common as an encrustation than it is in sample CW2. Poorly crystalline goethite forms a thin oxidized crust on part of the rock surface. Very minor amounts of a TiO_2 polymorph occur in the clay-rich part of the rock.

North Dump (NDP): Crumbly, mottled clay-rich rock (illite, kaolinite, montmorillonite)

with quartz, pyrite, goethite, relict feldspars, chlorite-rich segregations with chlorapatite, a TiO_2 polymorph, and zircon. Yellow jarosite forms clots within the rock and coats fractures. Jarosite grains are <10 μm across (more commonly 1-3 μm across) and contain low concentrations of P. Jarosite, intergrown with kaolinite, quartz, and alunite, forms soft orange-brown clots in the rock's interior. Thin laths of alunite also occur with euhedral-to-subhedral quartz as a fracture filling or, possibly, relict veins. An Fe-rich red crust, with minor amounts of S, Al, and Si, is locally present but uncommon. Just beneath the surface of this crust are found smooth cocci sheaths, <5 μm in diameter, that are compositionally similar to the crust. Grains, <15 μm across, of an APS with Pb, Ca, Ba, and K are uncommon. Sparse chocolate brown fragments have a morphology that is somewhat similar to, but not as symmetric as, the preserved plant material found in sample SAL-BS, described below. SEM-EDS gives a strong Fe + S (with minor P) signature.

N. Dexter-2 (ND2): Crumbly, porous clay-rich rock. The bulk of the rock is a mottled medium gray with irregular darker gray zones and yellow zones. Chalcanthite forms an efflorescent crust and thin veinlets. Chalcanthite grains are a clear medium blue and are coated by a lighter blue powder, presumably a dehydration product of the chalcanthite. Quartz and pyrite are disseminated and locally concentrated in a kaolinite + illite groundmass throughout the rock. Accessory minerals include anatase, APS minerals (svanbergite-woodhouseite solid solution with Ba and tentatively identified hinsdalite), tentatively identified enargite, and a phosphate mineral. Both illite and kaolinite are exceptionally well crystallized: illite forms euhedral hexagonal grains and kaolinite occurs in books of tabular hexagonal crystals, each crystal is <5 μm across. The dark gray zones contain concentrations of pyrite, anatase, and svanbergite-woodhouseite, together with quartz, kaolinite, illite, and trace amounts of a Ce- and La-rich phosphate mineral. The source of the yellow color in the yellow zones has not been identified. Secondary yellow minerals, such as jarosite and copiapite (an Fe-sulfate), were not found.

S. Pit-1 (SP-1): Sample SP-1 consists of two texturally distinct parts. One part is a finely laminated gray clay-rich rock with a uniform fine-grained texture. It is coherent. The surface is rippled and is non-uniformly coated with a thin medium brown crust, similar to those described above (samples TCOSP and MFCOSP; see text for discussion). The second part of the rock is crumbly and consists of gray clasts in a clay-rich groundmass. Quartz, illite, kaolinite, pyrite, relict grains of Ca- and Ba-bearing APS minerals, brown biotite, and TiO_2 polymorphs occur in both parts of the rock. Jarosite and lesser amounts of alunite are disseminated in the clay-rich groundmass and concentrated on the exposed surfaces. The gray clasts preserve a relict texture and consist of quartz, abundant pyrite, kaolinite, and illite; euhedral clay pseudomorphs after feldspar are common.

Area L Seep - Bank Seep (SAL-BS): Clay-rich rock (illite, kaolinite, smectite) with quartz and minor pyrite. Relict plagioclase, alkali feldspar, Ti-rich biotite, TiO_2 polymorph, svanbergite-woodhouseite solid solution, and uncommon alunite are present. The rock groundmass varies in color from dark to light orange and dark to light brown, differences which we attribute to different concentrations of Fe-rich minerals. Disseminated jarosite grains, 2-3 μm across, are more abundant in the orange groundmass than in the brown parts. Jarosite also occurs as surficial yellow encrustations on altered feldspar clasts with APS minerals that have a strong woodhouseite-svanbergite component. Poorly crystalline Fe-oxyhydroxide, with minor S and P, forms thin dark red-brown crusts on mineral clasts. Distinctive columnar brown fragments with a cellular structure indicative of preserved plant stems or twigs (Fig. 9A, B; D. A. Willard, USGS, personal communication, 1995) are found embedded in clay and are especially common in chocolate brown "clots," the color probably due to the presence of the plant relics. SEM-EDS indicates that the plant fragments have

been replaced by an Fe+S-rich phase with minor P and, in some occurrences, minor Cu. XRD analysis yielded a pattern typical of amorphous material with only a few very weak peaks. Aggregates of microspheres, possibly cocci, are associated with some preserved plant fragments. The presence of another Fe-rich, S±P, mineral is indicated by SEM-EDS data and weak peaks in XRD patterns, consistent with several of the Fe-hydroxides (ferrihydrite, goethite, schwertmannite), but a positive identification has not yet been made.

H_2O-treat (H_2O-t): Gray to white moderately coherent kaolinite- and illite-rich rock with embedded grains of quartz, pyrite, and K-feldspar. Soft orange aggregates of illite, goethite, and minor jarosite form clots in the interior. A dull yellow to yellow-green mineral, which is tentatively identified as sideronatrite, forms a somewhat nodular crust that partly coats the sample. The nodules are composed of thin (<0.5 μm thick) curved plates and scaly masses. Finely crystalline white sodium sulfate forms aggregates of orthorhombic plates that are concentrated in crevices formed by the yellow coating. Individual sodium sulfate grains are <5-10 μm across. Optical examination showed a yellow mineral associated with the sodium sulfate. SEM examination indicated that the yellow mineral is texturally and compositionally similar to the tentatively identified sideronatrite. SEM examination also indicated that at least two other sulfate(?) minerals are associated with the sodium sulfate: a prismatic phase with S, Na, Fe, and Mn and an anhedral phase with S, Al, and Na. Both of these minerals form grains < 10 μm across.

Stalactite from the Reynolds Tunnel

Stalactite-Adit 1500 (AD1500): The stalactite is an extremely porous and fragile tube with a maximum diameter of ~1.5 cm. Macroscopically, the color is a dull orange brown, but optical examination showed that the structure is composed of multiple, complex layers with different colors and textures. In cross-section, the stalactite is layered with relatively thin, hard dark red glossy layers interlaminated with thicker soft layers. The thicker layers are porous and appear fibrous or composed of fine networks of thin membranes with a variety of colors: dull pink-tan, red-brown, light or dark orange. The outermost layer of the stalactite is composed of a soft orange granular to powdery material that coats a thin red layer. When the layers were partly disaggregated, it was found that the red layers are not uniform but also have yellow and green zones.

SEM examination provided evidence for the role that bacteria may have played in the formation of the stalactite (Figs. 6A-E). All parts of the structure are dominated by aggregates of microspheres, morphologically similar to cocci. The microspheres are submicron to ~4 μm in diameter. Within different layers, the microspheres have different textures, form different structures, and have different compositions, as indicated by SEM-EDS. All compositions are dominated by Fe, with different amounts of S, P, and As. Si and Al may also be present. Thin smooth fragmented layers are found within the stalactite and are coated with microspheres; these smooth layers are compositionally similar to the microspheres. Other smooth red fragments are partly coated with fine micron-to-submicron-particles that are not morphologically distinct. STEM and XRD data indicate that the bulk composition of the stalactite is poorly crystalline two-line ferrihydrite. See text for discussion.